International Conference on Space Optics—ICSO 2022

Dubrovnik, Croatia

3–7 October 2022

Edited by Kyriaki Minoglou, Nikos Karafolas, and Bruno Cugny,

WDM Optical Front End for GEO-Ground Digital and Analog Telecommunications

International Conference on Space Optics — ICSO 2022, edited by Kyriaki Minoglou, Nikos Karafolas,
Bruno Cugny, Proc. of SPIE Vol. 12777, 127774C · © 2023 ESA and CNES · 0277-786X · doi: 10.1117/12.2690827

WDM Optical Front End for GEO-Ground Digital and Analog Telecommunications

C. Guyot*[a], J. Hauden [a], A. Laurent [b], T. Anfray[c], O. Pouzargues[c]
[a]iXblue Photonics, 3 rue Sophie Germain, 25000 Besançon, France; [b]iXblue Photonics, rue Paul Sabatier, 22300 Lannion, France; [c]Airbus Defence & Space, 31 rue des cosmonautes, 31402 Toulouse cedex, France

ABSTRACT

iXblue and Airbus Defence and Space developed a space-grade optical transceiver to increase communication rate between geostationary (GEO) or low earth orbit (LEO) satellites and earth. First demonstration model which will be launched early 2023 on a geostationary satellite possesses 2 downlink channels working at 10 Gb/s in non-return to zero differential phase shift keying (NRZ-DPSK), and 3 uplink demodulation channels. Two of them are dedicated to analog signals around 1 GHz, and one is dedicated for digital on-off keying (OOK) signal at 10 Gb/s.

Keywords: Transceiver, Space-grade, Telecommunication, electro-optical modulation, NRZ-OOK, NRZ-DPSK, analog

1. INTRODUCTION

In space, the data-rate standard transmission solutions using RF technology is limited. The need for high-speed communications, reaching the range of hundreds of Tbit/s creates an opportunity that can only be addressed by photonics-based solutions. The added advantages of photonics solutions in space are also reliability, even under harsh environment, scalability (modulations schemes, numbers of optical channels…) as well as smaller payload that reduces satellite consumption and data security against jamming.

In a previous work - Feeder Optical Link for Constellation (FOLC) - which was supported by the European Space Agency, a complete Optical Telecom Space bidirectional link system was implemented at breadboard level, including all the necessary hardware from Emitter (Tx) / Receiver (Rx) optical modules, High Power Optical Amplifier, Low Noise Optical Amplifier (LNOA), free space optical channel. The total capacities for the uplink and downlink were 176 Gb/s and 120 Gb/s respectively but only 75 Gb/s for each were emulated on the test bench. Channels multiplexing was based on a Wavelength Division Multiplexing (WDM) architecture of 25Gb/s channels in the 1539-1563 nm optical wavelength window. The aim was to manufacture evaluation breadboard of the optical communication chain using mainly parts selected for their future usage in space. In that frame we tested different scenarios of data encoding, namely 10Gb/s and 25Gb/s multiplexed channels in Non-Return to Zero Differential Phase Shift Keying (NRZ DPSK) and in Non-Return to Zero On-Off Keying (NRZ OOK). This work was reported in [1][2][3].

The current work of FOLC2 project is the continuation of FOLC and aims to design and manufacture a transceiver in a space-grade version. After the fabrication of an EM version to test the performances of the system in laboratory conditions, we built a space-grade demonstration model that will be installed on a GEO satellite inside a full optical terminal demonstrator called TELEO for a 2-year mission.

Actually, LCE (Laser Communication Equipment) or transceiver is part of a full Optical Board Terminal (OBT) composed also of a 26 cm diameter telescope, a focal plane, a high-power optical amplifier (HPOA), a Digital Process Unit (DPU) as shown in Figure 1. This paper focuses on the transceiver. More information on the overall communication chain performance can be found in [7].

*clement.guyot@ixblue.com; phone +33 1 30 08 88 88; ixblue.com

2. SYSTEM DESCRIPTION

LCE is assembled with space qualified processes and is composed by 3 different stages: a transmitter (Tx), a Receiver (Rx) and DC/DC converter stage (CV). These three stages have extended 6U dimensions. A backplane motherboard allows the communication between the 3 stage and DC supply of Tx and Rx boards. The dimensions of the demonstration model are 27 cm x 28 cm 10 cm. The manufactured equipment is presented in Figure 2.

All the connectors are on the front panel side of the transceiver. Bottom floor is the transmitter and possesses 2 SMK RF input connectors and an output PM optical fiber. Middle floor is the CV board and possesses a 100V DC supply D-click connector and a D-click connector dedicated to communication for send TM/TC (Telecontrol/Telemetry). Eventually, top floor is the receiver board and possesses a single mode input fiber, and 6 RF SMPM outputs for the three installed photoreceivers. After mounting cables from DPU to photoreceiver SMPM connectors, a mechanical flange is fixed to consolidate RF cable holding.

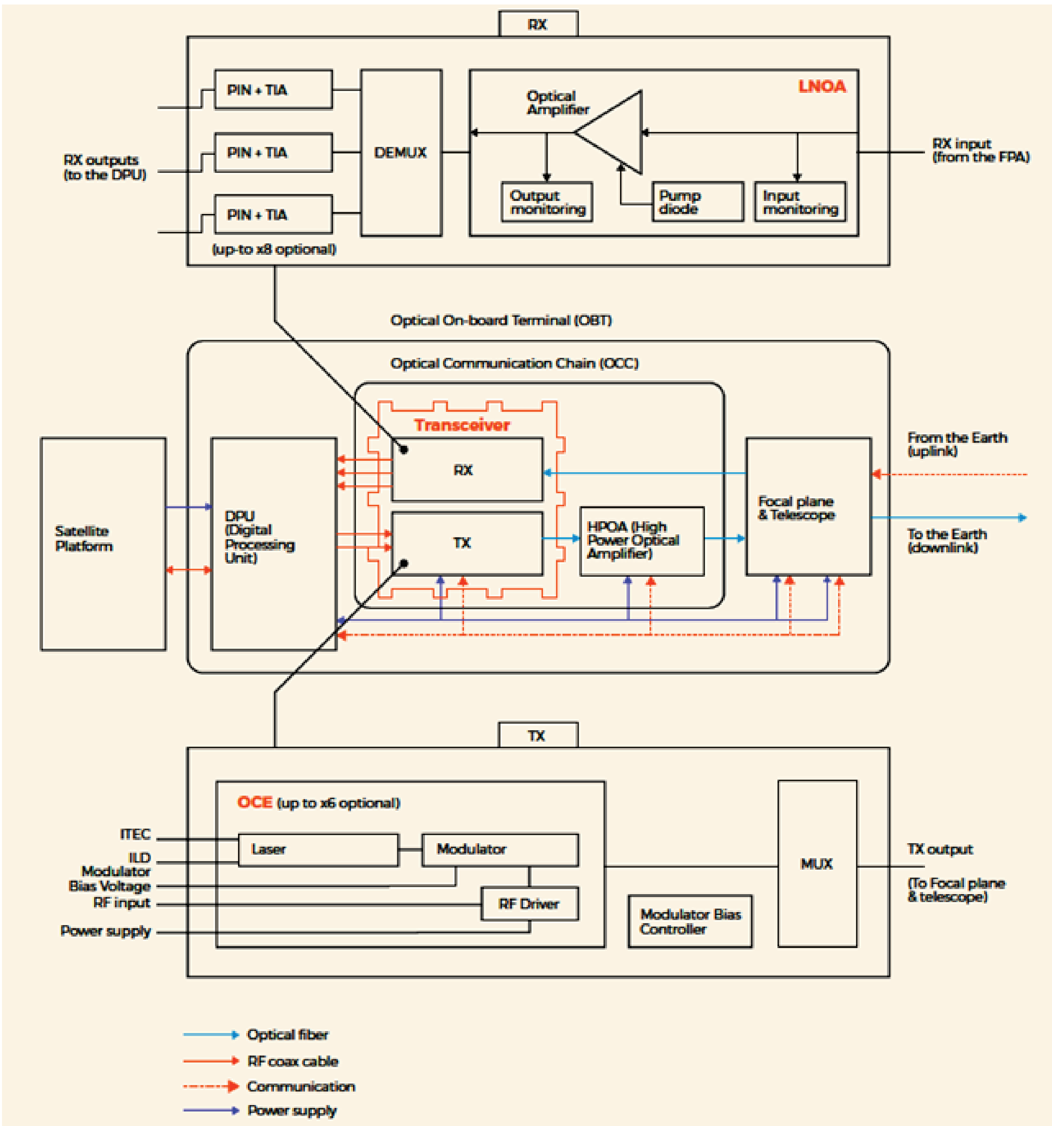

Figure 1. Optical Board Terminal synoptics (middle). Schemes of the Rx (top) and Tx (bottom) stages of the transceiver.

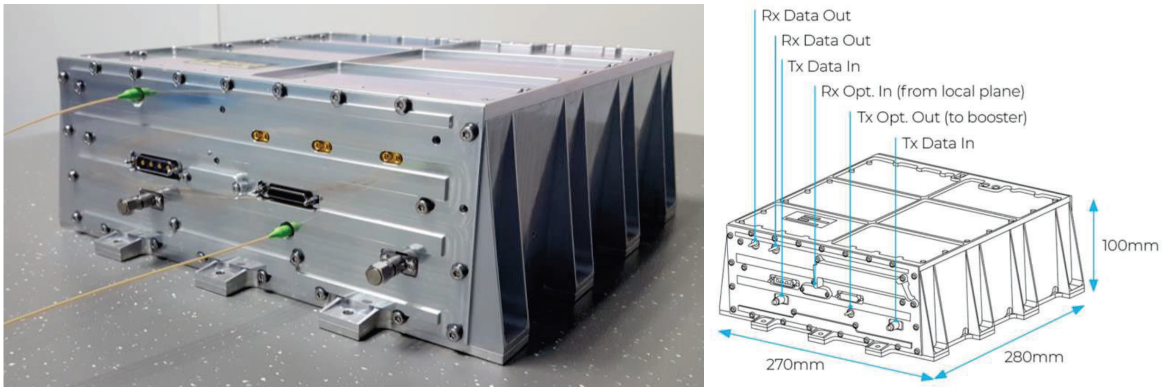

Figure 2. Transceiver demonstration model photography and scheme

2.1 Transmitter stage

The transmitter is composed of two modulated optical channels (one nominal and one in cold redundancy) that are multiplexed through a 50/50 PM fiber coupler. Each modulated signal is produced by an Optical Channel Emitter (OCE) that is detailed below. OCE output powers are monitored by a photodiode, which allow for the control of the modulator bias voltages. Tx optical output is a PM fiber protected by PEEK jacket. It is terminated with a space-grade Mini-Avim FC/APC connector.

Optical Channel Emitter
The optical channel emitter (OCE) is a standalone product including all the required components to generate high speed optical data signal in the 1550nm window. It is composed of a Distributed Feedback Laser, a space-grade high speed MZM (Mach-Zehnder modulator) and a space-grade RF broadband amplifier. OCEs that have been installed in the LCE of TELEO demonstrator are dedicated to NRZ-DPSK modulation format at 10 Gb/s. The OCE dimensions are 10 x 6 x 2 cm^3. The OCE, shown in Figure 3, includes a SMK RF input, an optical PM fiber output and an electrical connector for the power supply and the control.

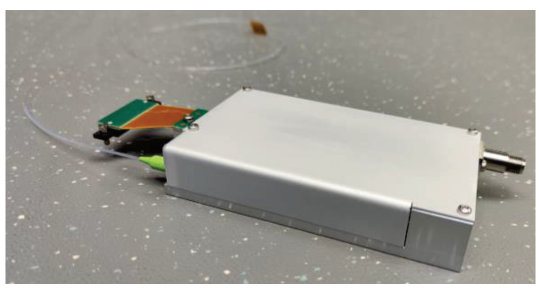

Figure 3. Picture of a space grade 10 Gb/s NRZ-DPSK OCE

191.8 and 192 THz DFB lasers with maximum operating output power of 16 dBm have been selected. OCE Optical output power can reach 13 dBm before any derating consideration and is error free without signal attenuation.

Lithium niobate electro-optical modulators (MZM) have been chosen as a reliable technology in harsh environment and for their performances (low insertion losses, high dynamic extinction ratio and high data rate capacity) [4][5]. Dedicated modulators SP-MX-LN-20 based on iXblue space-grade modulator heritage have been designed and manufactured to fit in OCE size. Typical DC half-wave voltage is 5.8 V and RF half-wave voltage is 5.4V at 50 kHz. Static Extinction Ratio is higher than 20 dB and electro-optical bandwidth is greater than 20 GHz.

Space-grade RF amplifiers have been designed and manufactured in partnership with Airbus Defence and Space. They are based on a combination of different RF-chips (hybridation). Special care has been taken in the selection of the RF chips and their assembly so as to ensure a good thermal dissipation while respecting junction temperatures and voltages deratings. Their role is to adapt the voltage swings form the electric Telecom signals (around 250 mVpp) to the required input voltages of the MZM (around 11 Vpp to 12 Vpp). In the NRZ-DPSK version, the RF amplifiers exhibit a 44dB gain and can accept input amplitude from 150 to 400 mVpp.

Figure 4 bellow shows the back-to-back NRZ-DPSK optical eye diagrams at 10Gb/s recorded at the output of the OCE and the electrical eye diagram after demodulation thanks to a delay line interferometer and a balanced photoreceiver. The data are 2^{31}-1 long pseudo-random sequence (PRBS). After demodulation Electrical Signal to Noise Ratio (ESNR) is close to 14 for all the manufactured OCEs.

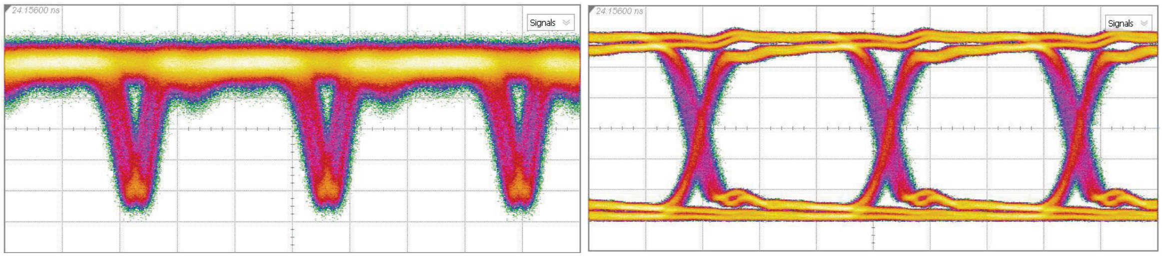

Figure 4. (left) 2^{31}-1 PRBS 10G/s DPSK eye diagram and (right) demodulated DPSK eye diagram.

2.2 Receiver stage

The receiver is composed of a Low Noise Optical Amplifier (LNOA), a demultiplexer and three high-speed photoreceivers. Two photoreceivers are dedicated to analog links (one being used as a redundancy) and one is used for digital link. Digital format is NRZ On-Off Keying (NRZ-OOK) and data rate is up to 10 Gb/s.

LNOA: Low noise optical amplifier, shown in Figure 5, is a radiation hardened Erbium active fiber-based solution with 37 dB of gain. LNOA dimensions are 11 x 7 x 2 cm^3. The LNOA has been optimized to get a low noise factor at single wavelength or with 3 WDM signals in the range of 193.4 to 193.8 THz. LNOA front panel presents single mode input and output fibers, an electrical connector. End of life consumption is lower than 0.5 W. An interstage filtering is realized thanks to dedicated space qualified home-made fiber Bragg gratings in order to optimize the noise factor (NF).

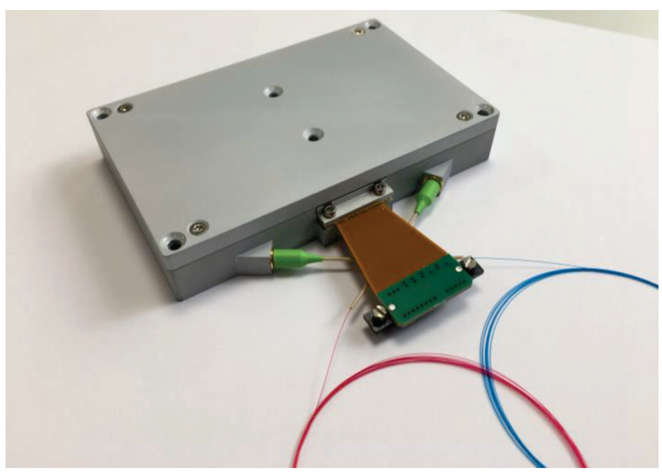

Figure 5. Photography of LNOA.

Figure 6 presents typical performances of the LNOA. At 5°C and 25°C, for each of the 3 Wavelength Division Multiplexed channels (WDM) the optical gain is between 36 and 37 dB. At temperatures higher than 60°C, a 3dB decrease is observed.

Between 5 and 62°C, the noise factor (NF) is comprised between 3.7 and 4 dB for received optical power (ROP) varying from -50 to -20 dBm. For lower input power (55dBm) NF decrease is mainly explained by measurement imprecision and noise. Let us note that these results do not include the insertion losses of the LNOA input tap coupler used for the input optical monitoring. The presence of this optional splitter induces a 1.68 dB increase of the NF.

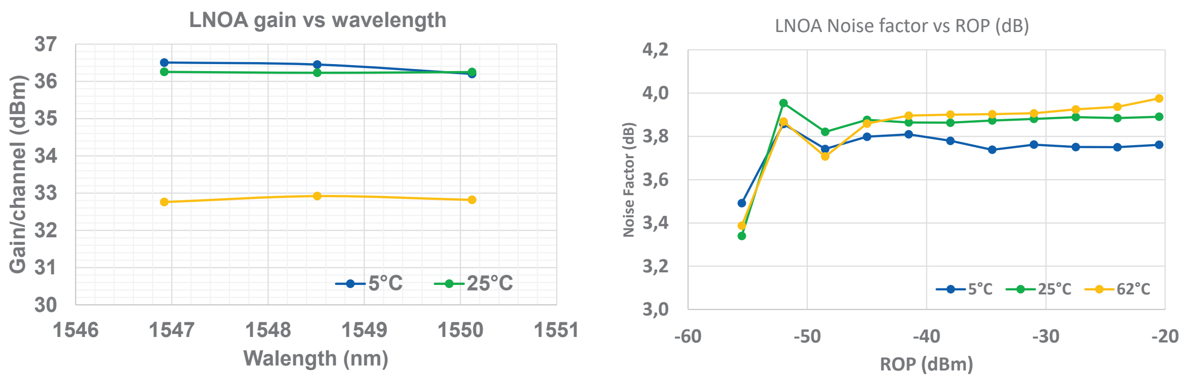

Figure 6. (left) Measured gain per channel vs wavelength at different temperatures. (right) Noise Factor vs ROP at different temperature in WDM.

Demultiplexer: At LNOA output, the amplified signal goes through a 3-channel fibered demultiplexer. This demultiplexer is realized with customized Fiber Bragg gratings manufactured by iXblue and commercially of the shelf (COTS) fibered passive optical components (splitters and circulators). The demultiplexer optical output spectrum is shown in Figure 7. At optimized frequency and room temperature, for every channel, the insertions losses are comprised between 3.5 and 3.9 dB, inter-channel isolations are higher than 35 dB and full width at half maximum are 140 GHz.

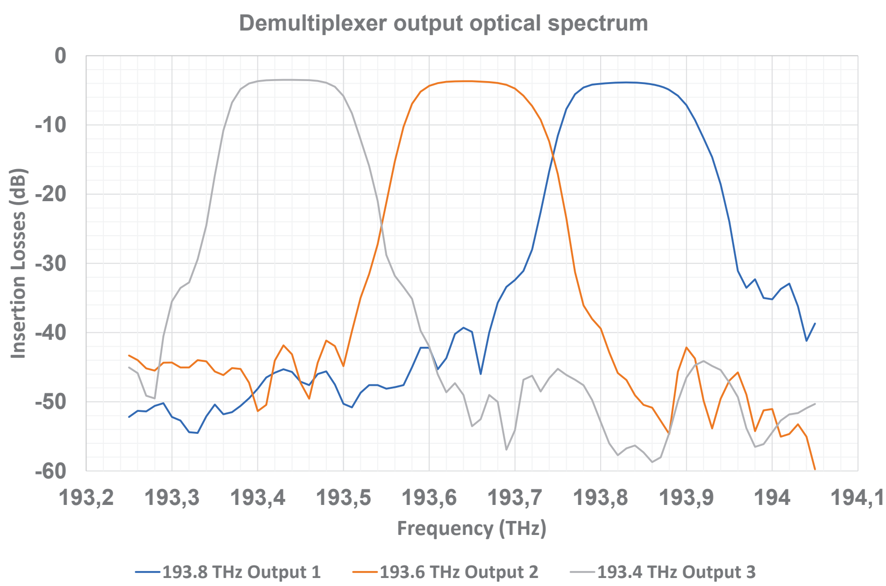

Figure 7. Recorded demultiplexer output optical spectrum.

The selected photoreceivers (or OCR - Optical Channel Receiver) are composed of high- speed photodiodes with a 2-stages transimpedance amplifier (TIA). A unique reference has been chosen for both analog and digital applications and the manual gain of the TIA second stage is adjusted to work either in linear region for analog demodulation or in saturation region for digital demodulation. This reference possesses two SMPM RF outputs and works in differential mode. The typical differential conversion gain is 1500 V/W and maximum output voltage is 1.8 Vpp. Consumption of each photoreceiver is lower than 0.3 W.

3. SYSTEM PERFORMANCES AT AMBIENT PRESSURE

The system has been fully measured at +20°C, +10°C and +59°C which correspond to qualification temperatures (±10°C margin compared to mission temperature range).

Transmitter

With one active channel at a time, OCE are set up for the Tx to deliver an output power of 7 dBm, which fits with HPOA necessary input power. Minimum polarization ratio is higher than 20dB whatever the active channel, for a minimum requested PER of 16dB.

Figure 8 shows typical Bit Error Rate (BER) depending on Received Optical Power for one active channel at 10 Gb/s with 2^{31}-1 PRBS signals. BER is evaluated with a BER-Tester. Attenuation at Tx output is tuned thanks to a Variable Optical Attenuator (VOA) so as to modify the ROP. The receiver is composed of a simple high speed photoreceiver without LNOA and DEMUX. Tx is error free without attenuation. At room temperature and at +10°C, apparition of first errors could be observed for optical power of -11 dBm. The 10^{-3} BER threshold is obtained for a received optical power of -15.5 dBm. A penalty of 0.6 dB in the ROP is observed at +59°C to reach 10^{-3} BER.

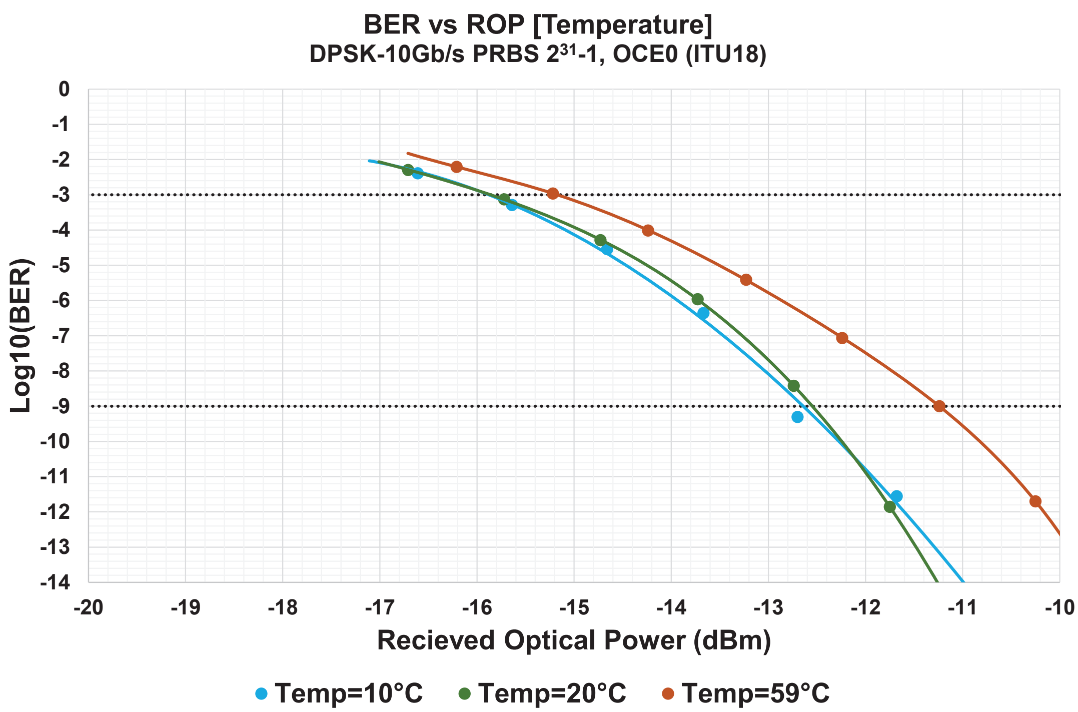

Figure 8. BER vs ROP at Tx output at ambient pressure and for different temperatures.

Receiver

For the analog channels, an analog modulated optical input signal is generated at a frequency of 1 GHz thanks to an electro-optical modulator and a RF synthesizer. This signal is injected in the Rx stage input fiber after attenuation through a VOA. Tunable laser has been used to select OCR-1 and OCR-2 center frequencies: 193.4 and 193.6 THz.

The RF power at photoreceiver SMPM single output connector is measured depending on the received optical power that enter the LNOA input. RF load is added on the unused RF output side. Photoreceiver gain has been set to get the best linear behavior. In Figure 9, we present this result for nominal channel (OCR2) at room temperature. Linearity is observed for ROP between -60 and -40 dBm.

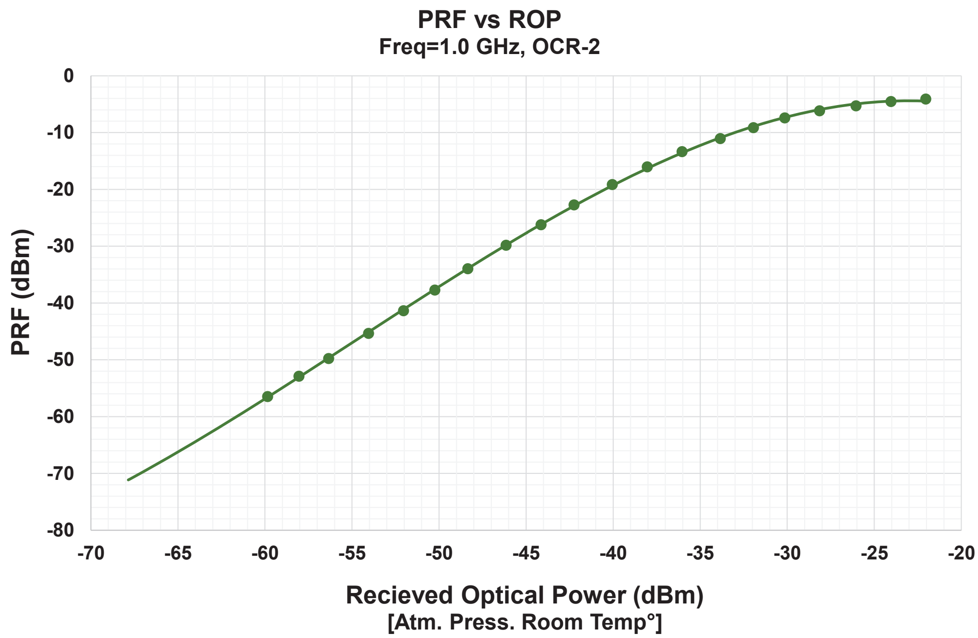

Figure 9. LCE Rx analog channel PRF vs ROP at ambient pressure and at +20°C

For Rx digital channel, the input signal consists in a 10 Gb/s OOK modulated optical signal at 193.8 THz. Length of PRBS is 2^{31}-1. Photoreceiver manual gain is set at its maximum for digital applications. Results are presented in Figure 10. 10^{-3} BER is obtained for a ROP of -43.5 dBm for the 3 tested temperatures. This is better than specification that requires a 10^{-3} BER for ROP of -41.5 dBm. A dispersion of approximately 1 dB can be noticed at 10^{-12} error rate.

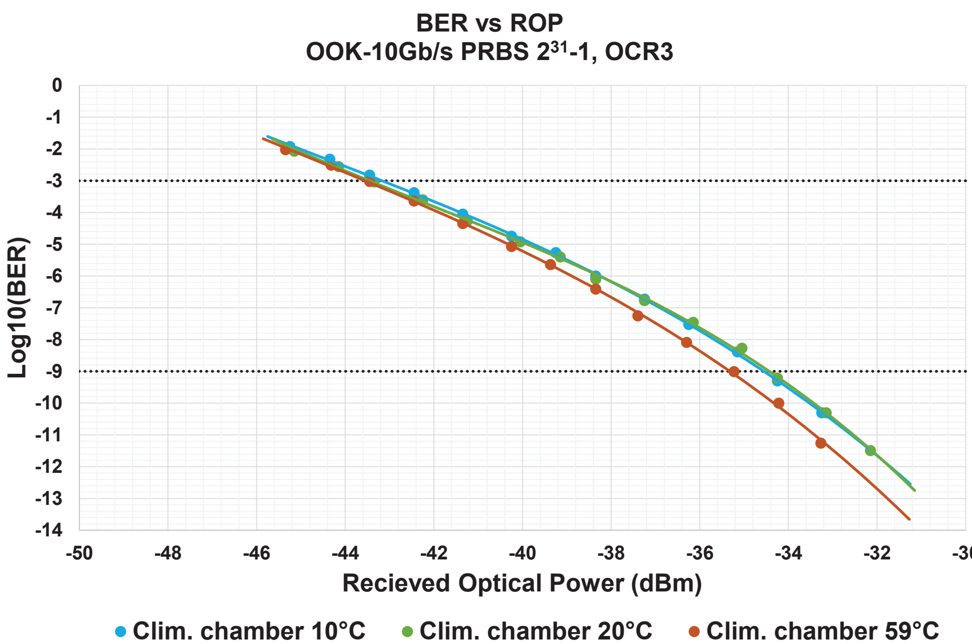

Figure 10. LCE Rx digital channel bit error rate vs ROP at ambient pressure and at different temperatures.

4. SYSTEM QUALIFICATION

4.1 Thermal vacuum cycling

LCE has been tested under vacuum (10^{-6} hPa) at qualification temperatures to check its performances in representative conditions.

After initial tests at +20°C under vacuum, the turned-off equipment saw a first temperature cycle at non-operating temperatures. After turning on the equipment, three thermal cycles have been done at operating temperatures. Performances have been measured at +10°C, +20°C and +59°C which are qualification temperature limits.

Transmitter

Wavelength and power stabilities, polarization extinction ratio, eye diagram and bit error rate have been measured on both OCE of the Tx board. Figure 11 shows the experimental setup for Tx measurements under vacuum.

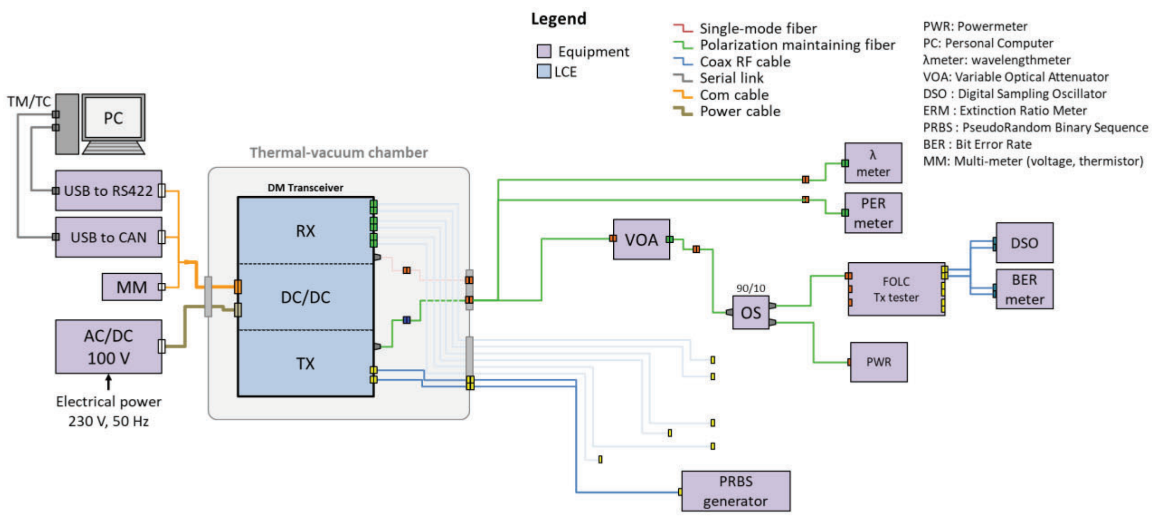

Figure 11. Tx board measurement experimental setup

During the thermal cycles, the optical power variation was ±0.1dB for both channels and the central optical wavelengths of both OCE varied only by 2 GHz which is lower than ±3.6 GHz allowed variation. Next figure shows the BER vs ROP under vacuum for a temperature of 20°Cat equipment TRP (temperature reference point) before and after thermal cycling. No evolution has been noticed. The results are similar to those observed at atmospheric pressure. 10^{-3} BER is reached for a ROP of -16 dBm

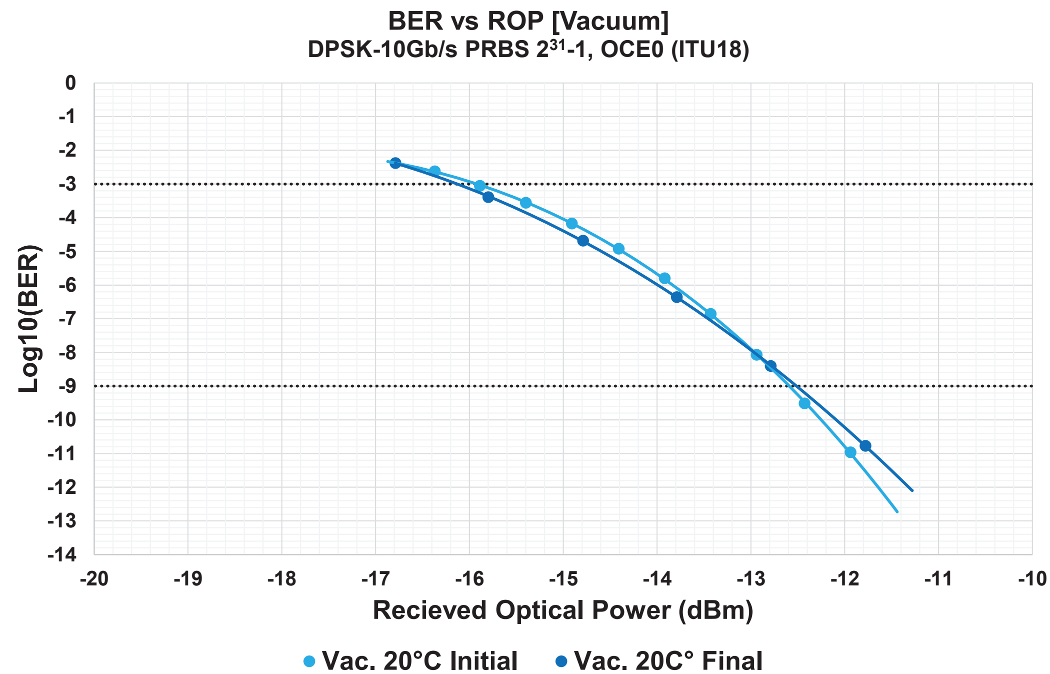

Figure 12. LCE Tx bit error rate vs ROP in vacuum chamber at +20°C. Initial and final means before and after thermal cycling under vacuum.

For the analog links, RF power at the output of photoreceivers depending on ROP has been measured to check the linearity of the response. The experimental setup is presented in Figure 13.

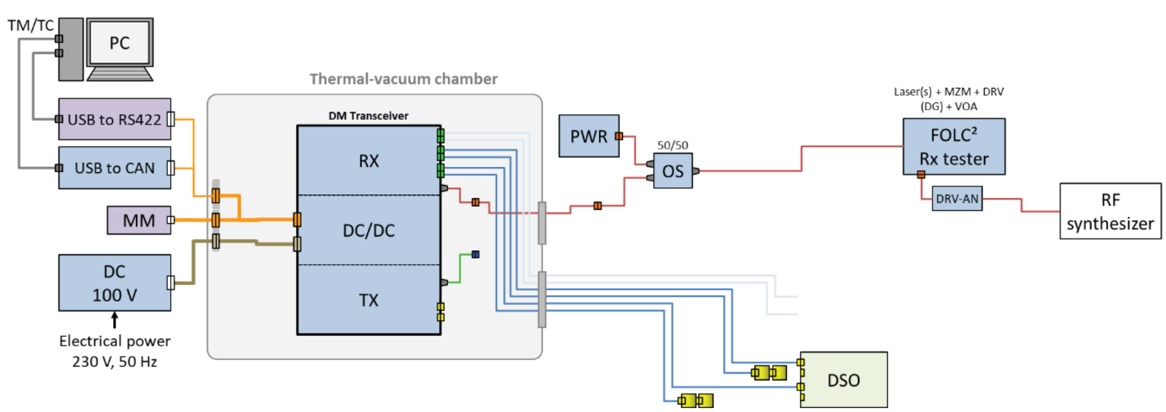

Figure 13. LCE Rx measurement setup for analog channels under vacuum.

Results are presented in Figure 14. Linearity is observed for ROP between -60 and -40 dBm. RF Response at photoreceiver output is similar for +10 and +20°C. It is however possible to see a shift of 2 dB at 59°C showing that gain start to be significantly degraded with temperature.

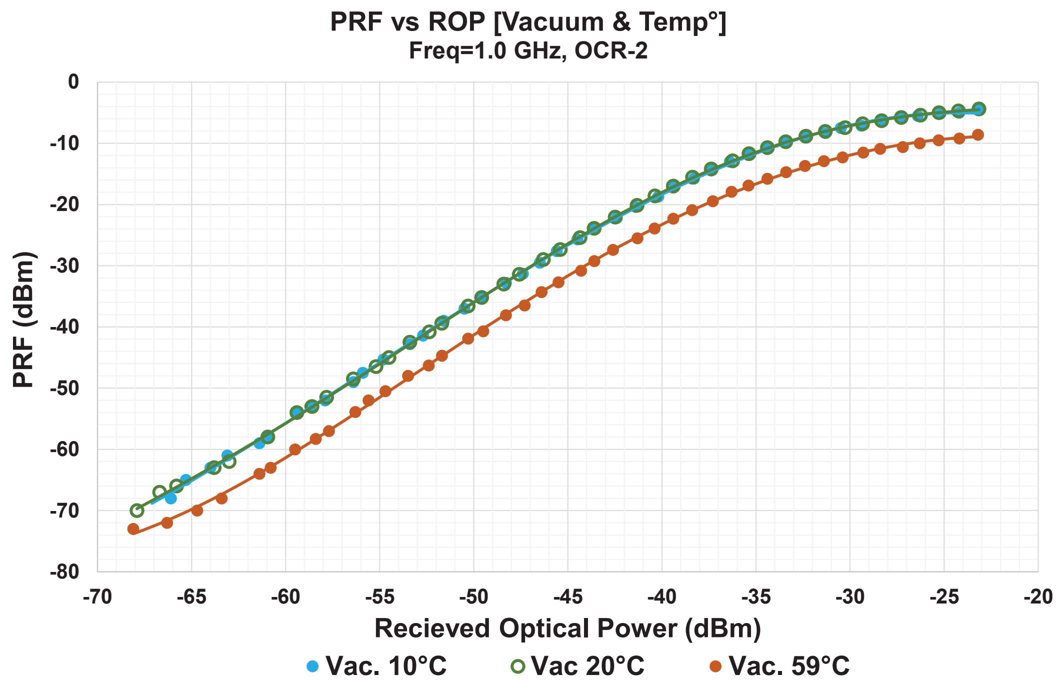

Figure 14. LCE Rx analog channel PRF vs ROP in vacuum chamber and at different temperatures.

For Rx board digital channel, characterizations lie on BER vs ROP measurements and eye diagram evaluations. Experimental setup is presented in Figure 15.

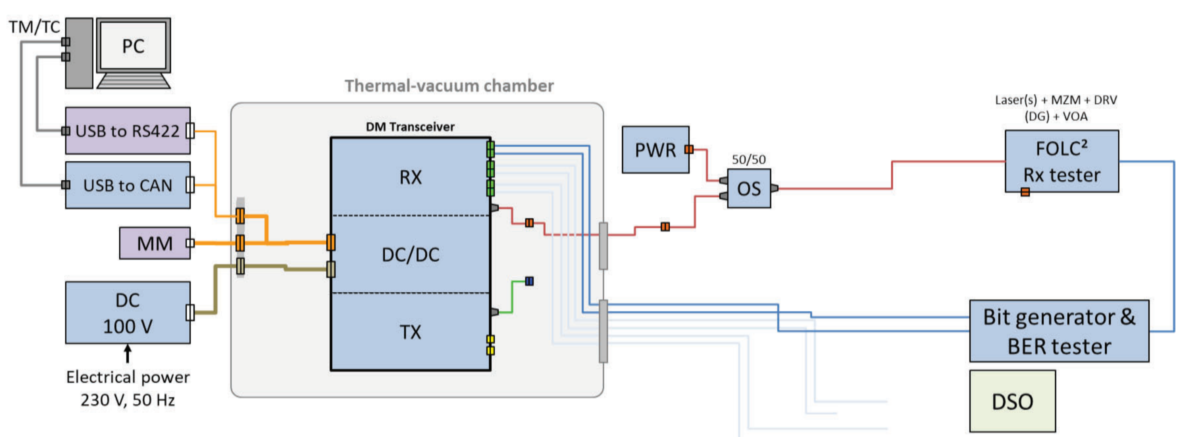

Figure 15. LCE Rx digital channel measurement setup under vacuum.

Bit error rate of 10^{-3} is observed for a ROP of -43.2 dBm whatever the temperature at TRP, as shown in figure 16. When compared to results at ambient pressure (Figure 10), we can notice that 10^{-3} BER is obtained at the same ROP under vacuum and at ambient pressure.

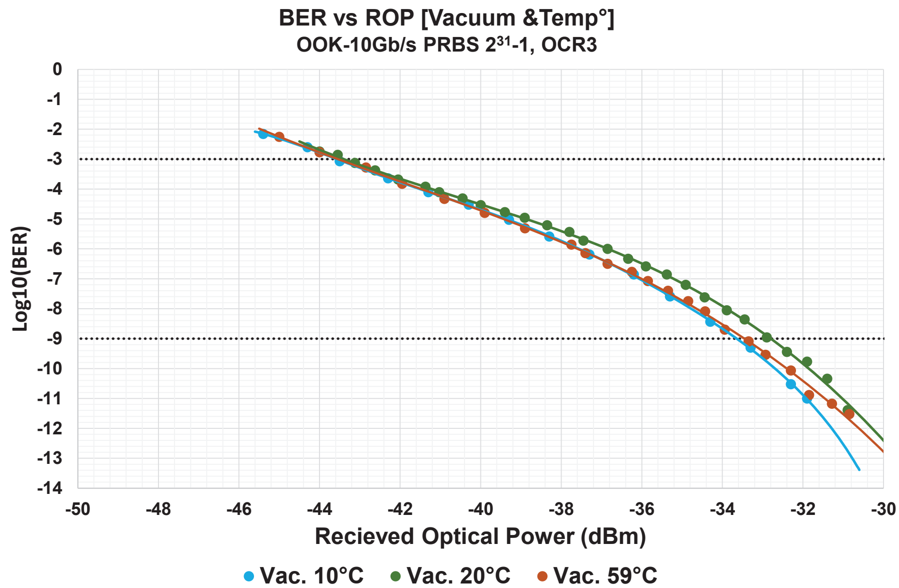

Figure 16. LCE Rx digital channel bit error rate vs ROP in vacuum chamber and at different temperatures.

4.2 Vibration and shocks

The equipment has undergone shocks and vibrations similar to launch. The equipment behavior has been tested after low frequency sinusoidal vibrations, quasi-static, and random ones. Random vibrations were made at a level of 9.5 g rms on axes parallel to the mounting plane, and 18.3 g rms on the perpendicular axis.

After vibrations, the equipment has been shocked by hammer shock method at 500 g on each axis.

Partial measurements have been performed on the equipment between vibrations and shocks to ensure its good health. The following parameters have been measured during mechanical tests:

- Output power and consumption of each OCE without modulation.
- Consumption of the entire Rx board

No performance evolution could be observed as shown in following Table 1.

Table 1. performance evolution during mechanical tests.

Item	Unit	Before vibrations	Between vibrations & shocks	After shocks
Tx P_{out} channel 0	dBm	7.57	7.54	7.55
Tx P_{out} channel 1	dBm	7.71	7.7	7.68
OCE0 consumption	W	19.2	19.3	19.2
OCE1 consumption	W	19.4	19.5	19.5
Consumption of LNOA and all OCRs	W	15.8	15.8	15.8

4.3 Component & sub-systems qualification

Qualification at system level does not include ageing, radiations, or long-term thermal cycling. These complementary qualifications have been done at sub-system or component level depending on qualification legacy and component criticalness. New space philosophy has been followed for optical components. Such considered new space philosophy for optical component qualification is detailed in [6].

Concerning radiations, simulations have been realized to determine expected TID and TNID for LEO and GEO missions. A worst case of 50 krad has been hypothesized for TID, and a maximum dose of 10^{11} p+/cm² is expected for TNID. All optical or electro-optical components have been tested in TID, and TNID will be done before the end of the year.

OCE and LNOA which are sub-assemblies of COTS and space-grade components requires complementary qualification. For instance, both products will undergo at the end of 2022 vibrations of 50 g rms and shocks up to 2000g on each axis.

5. CONCLUSION

A first space-grade optical transceiver co-developed by iXblue, and Airbus Defence & Space has been manufactured and tested. Optical building blocks have been designed to easily change the number of channels in transmitter or receiver, inducing major changes only in electronics and mechanical structure. A first demonstrator is qualified for a 2-year GEO mission. It is scheduled to be in orbit in 2023.

The Tx and Rx boards that have been developed are generic. There are transposable without drastic changes for different input/output channel wavelengths. Downlink data rate can be increased by replacing 10 Gb/s OCE by 25 Gb/s versions. Increasing uplink digital data rate would require a new reference of photoreceiver as preliminary tests showed a significant penalty at 25 Gb/s with current reference.

Increasing transmitter or receiver channel number will require a re-design mechanical part to accept supplementary Tx or Rx boards. The increase of channel number will also require new component to multiplex/demultiplex without increasing insertion losses inside the equipment. The typical arrayed waveguide grating MUX/DEMUX are currently in qualification process.

We gratefully acknowledge CNES (French Space Agency) and European Space Agency which supported financially and technically this project.

REFERENCES

[1] J. Hauden “From photonic components to transceivers”, EPIC Meeting on New Space at ESA 2019, 12-13 September 2019, Noordwijk, The Netherlands

[2] S. Mariojouls, T. Anfray, P. Berceau, L. Blarre, J. Hauden, A. Mottet, H. Porte, J. Bonnefoy, A. Laurent, T. Schmitt, R. Cousty, "Laser Communication Technologies for Space Applications", IEEE Photonics Conferences 2019, invited conference, Special Symposium on Space Photonics, 29 Sept- 3 Oct. 2019, San Antonio, USA, (SS SP)

[3] T. Anfray, J. Hulin, S. Poulenard, P. Berceau, S. Mariojouls, L. Blarre, W. Atitallah, A. Mottet, A. Laurent, J.-J. Bonnefois, J. Hauden, H. Porte, T. Schmitt, R. Cousty. "Assessment of the performance of DPSK and OOK modulations at 25 Gb/s for satellite-based optical communications", ICSOS 2019, 14-16 Oct. 2019, Portland Oregon, USA

[4] P. Crochet, J. Tchahame, “Optical Fibers and LiNbO3 Modulators for Space Applications”, Paris Space Week, February 25 - 26, 2020

[5] J. Tchahame, N. Grossard, J. Hauden, "LiNbO3 Modulators qualified for space applications", 28th European Symposium on Reliability of Electron Devices, Failure Physics and Analysis, ESREF 2017, 25-28 Sept 2017, Bordeaux, France

[6] L. Bouet, S. Mariojouls, A. Salomon, C. Guyot, J. Tchahame, A. Laurent, S. Ustaze, R. Cousty, T. Schmitt, Optoelectronics parts NewSpace qualification aboard FOLC2 optical modem mission, ICSO 2022, 3-7 oct. 2022, Zubrovnik, Croatia

[7] Sylvain Poulenard, Thomas Anfray, Michael Crosnier, Jean-Frédéric Chouteau, Jor-dane Thouras, Charles-Ugo Piat, Jean-Adrien Vernhes, Laurent Coret, Walid Atitallah, Alassane Dupuy, Louis Barbier, Lyonel Barthe, Benjamin Gadat, Thomas Dreischer, Etienne Samain, Erick Bondoux, Thierry Lanz, Fredéric Lacoste, Julien Sommer, “10 Gbauds digital optical link and analog link from/to geostationary satellite”, ICSO 2022.